The Open Biotechnology Journal
DOI: 10.2174/0118740707483472261006060307, 2026, 20, e18740707483472
ISSN: 1874-0707

RESEARCH ARTICLE **OPEN ACCESS**

Promising Intravitreal Retina-targeting and Immune-evading Adeno-associated Virus Capsid Variant: Preliminary Study

Zhongshan Cai[1,2], Yawen Liu[2], Li Zhao[2], Xiaofang Li[2], Binwu Zhang[2], Yuxu Tang[2], Tao Zhou[3], Zhuxia Zheng[3], Aonan Li[3], Jiye Wei[3], Qingzhou Ji[2,*], Daru Lu[1,*] and Damien Marsic[2,4,*]

[1]*MOE Engineering Research Center of Gene Technology, Obstetrics and Gynecology Hospital, Fudan University, Shanghai, China*
[2]*Porton Advanced Solutions, 388 Xinping St, Suzhou Industrial Park, Jiangsu, China*
[3]*ViewGene Therapeutics, 1 Hua Yun Rd, Suzhou Industrial Park, Jiangsu, China*
[4]*MaiBo Biotech, 1 Hanlin Rd, Suzhou Industrial Park, Jiangsu, China*

Abstract:

Introduction/objective: Retinal diseases are an important focus of *in vivo* gene therapy, for which adeno-associated virus (AAV) is a preferred vector. Intravitreal injection is a highly desirable delivery route because it is simpler, safer, and less expensive than the main alternative, subretinal injection. However, existing capsids have low efficiency, require high doses, and are susceptible to neutralization by antibodies that are present in the vitreous.

Methods: We developed a novel AAV capsid with improved properties to address these issues. Using AAV5 as starting material, we applied a combination of directed evolution and rational design to develop PT1, a novel capsid capable of transducing the retina after intravitreal injection.

Results: Compared to its parent capsid AAV5, PT1 has 15 surface amino acid substitutions in five variable regions and has its VP1-unique region swapped with that of AAV8. Its production yield is similar to that of another AAV5-derived control capsid and superior to that of AAV2. PT1 could transduce the retina-derived cell line ARPE-19 as efficiently as control retinal capsids and with better specificity than AAV2. PT1 performed exceptionally well in an *in vitro* immune evasion assay, largely surpassing control capsids. *In vivo* transduction following intravitreal injection in mice suggested strong specificity for Müller glia cells.

Discussion: PT1's most striking property is its ability to evade preexisting neutralizing antibodies (NABs), apparently thanks to its multiple mutations spread over large areas of the capsid surface, disrupting several epitopes. Another interesting property is its apparent specificity for Müller glial cells, an important therapeutic target. Both of these properties are based on limited evidence and will require further experimental confirmation.

Conclusion: The results of our preliminary study suggest that PT1 could become a useful addition to the current retinal AAV capsid toolkit, should future studies confirm our findings.

Keywords: AAV, Capsid, Intravitreal, Retina, Immune evasion, Müller glia.

© 2026 The Author(s). Published by Bentham Open.
This is an open access article distributed under the terms of the Creative Commons Attribution 4.0 International Public License (CC-BY 4.0), a copy of which is available at: https://creativecommons.org/licenses/by/4.0/legalcode. This license permits unrestricted use, distribution, and reproduction in any medium, provided the original author and source are credited.

*Address correspondence to these authors at the MOE Engineering Research Center of Gene Technology, Obstetrics and Gynecology Hospital, Fudan University, Shanghai, China, Porton Advanced Solutions, 388 Xinping St, Suzhou Industrial Park, Jiangsu, China and MaiBo Biotech, 1 Hanlin Rd, Suzhou Industrial Park, Jiangsu; E-mails: damien.marsic@gmail.com, qingzhou.ji@portonadvanced.com and drlu@fudan.edu.cn

Cite as: Cai Z, Liu Y, Zhao L, Li X, Zhang B, Tang Y, Zhou T, Zheng Z, Li A, Wei J, Ji Q, Lu D, Marsic D. Promising Intravitreal Retina-targeting and Immune-evading Adeno-associated Virus Capsid Variant: Preliminary Study. Open Biotechnol J, 2026; 20: e18740707483472. http://dx.doi.org/10.2174/0118740707483472261006060307

Received: March 26, 2026
Revised: August 24, 2026
Accepted: September 01, 2026
Published: October 13, 2026

Send Orders for Reprints to reprints@benthamscience.net

1. INTRODUCTION

Adeno-associated virus (AAV) has emerged as the viral vector of choice for human *in vivo* gene therapy in both clinical trials and approved therapies [1]. The eye, and more specifically the retina, is a particularly important target for gene therapy, representing 23% of all AAV-mediated clinical trials [2]. Luxturna, which uses a wild-type AAV2 capsid, is the only approved retinal gene therapy so far [3]. It is delivered by subretinal injection, a complex surgical procedure requiring hospitalization. The main alternative to subretinal delivery is intravitreal injection, which is a simpler and safer procedure that can be performed in an office setting. The reason why subretinal injection has been favored so far is that it's much more efficient. Very few capsid serotypes are capable of transducing the retina when injected intravitreally, and those require large doses (typically two orders of magnitude higher than *via* the subretinal route) to compensate for the lower efficiency. In addition, while the subretinal space is immune-privileged, the vitreous contains potentially neutralizing antibodies [4], requiring patients to be screened and eventually excluded from receiving the gene therapy if they have high titers of antibodies neutralizing the capsid being used. On the other hand, intravitreal injection has the advantage of targeting a larger area of the retina, while the viral vectors injected subretinally tend to transduce a smaller area at the injection location.

Since there is no selective pressure in nature to evolve capsids into efficient gene therapy vectors, efforts have been made during the past two decades to develop engineered capsids with improved properties, using a range of approaches including directed evolution, rational design, or a combination of both [1, 5, 6]. The property that attracted the most attention is the ability to efficiently target specific tissues or cell populations *via* a particular administration route, by modifying the capsid surface to disrupt or promote interactions with cell surface receptors [7-9]. Another important property is transduction efficiency, which can be improved independently of tissue specificity, by enhancing the capsid's ability to evade degradation after cell entry [10]. Not much effort has been put, in the field of retinal gene therapy, into developing capsids able to evade preexisting NABs, with the property emerging just as a side effect of introducing surface mutations to alter tropism [9]. Finally, another property that can be affected by capsid engineering is the efficiency of capsid assembly. Unlike with other properties, capsid engineering is unlikely to improve what has already been optimized by natural selection; on the contrary, each alteration of the capsid amino acid sequence risks adversely affecting the ability of the monomers to fold correctly and assemble into a functioning capsid, resulting in a lower AAV production yield. Considering the high costs of producing AAV, novel engineered capsids with enhanced tissue specificity or transduction efficiency therefore also need to be evaluated for the ability to produce AAV with a reasonable yield.

Progress has been incremental so far, and much more work is needed to make ocular gene therapy more accessible. The development of novel AAV capsids capable of more efficiently transducing retinal tissue after intravitreal injection while successfully evading preexisting NABs will make retinal gene therapy safer, cheaper, and accessible to larger patient populations.

Here we introduce a new AAV capsid variant resulting from a combination of incremental directed evolution and rational design, with a large number of mutations across wide areas of the capsid surface, capable of transducing retinal tissue and with a remarkable ability to evade preexisting NABs.

2. MATERIALS AND METHODS

2.1. AAV Capsid Libraries

Capsid libraries were designed and constructed as described previously [11, 12]. The original library used in NHP was based on AAV5, while the library used in mice was based on a variant enriched from the original library. All libraries, including before and after enrichment, were analyzed using Illumina 2x150 paired-end sequencing. The nucleotide sequences of the diversified regions of the capsid libraries, as well as their amino acid translations, are shown as supplementary material in the repository referenced in the Data availability section.

2.2. Control Capsid Sequences

All control capsid genes were recreated from published sequences using standard molecular biology techniques (Gibson assembly of PCR fragments generated using synthetic oligonucleotides). For LSV1, which was unpublished, the sequence was copied from related patent US11510950B2 [13].

2.3. AAV Preparations

Recombinant AAVs were prepared using triple plasmid transfection of adherent AAV-293 cells and purified by iodixanol (OptiPrep, Sigma-Aldrich) gradient centrifugation as previously described [14]. The plasmid containing the GFP-encoding recombinant genome was pAAV-GFP [15]. When high endotoxin levels (>10 EU/ml) were detected, an additional endotoxin removal step [16] was performed, involving incubation in 0.5% Triton X-100 (Sigma-Aldrich) followed by repeated buffer-exchange washing and concentrating using centrifugal concentrators (Sartorius Vivaspin 20).

2.4. AAV Quantification

Two µl AAV samples were first treated with DNase I (Vazyme Biotech, China) for 10 minutes at 37°C in a 20 µl volume. DNase was then inactivated by incubating at 75°C for 10 minutes in the presence of 25 mM EDTA. An equal volume of AAV lysis buffer (0.55 SDS, 20 mM Tris pH 8.0, 2 mM EDTA) was then added to each reaction, which was incubated at 70°C for 10 minutes. Samples were then further 50x diluted before being used as qPCR templates. The probe method was used to perform qPCR, with a linearized plasmid as the standard. Primers were ITR-F:

5’-GGAACCCCTAGTGATGGAGTT and ITR-R: 5’-CGGCCTCAGTGAGCGA. The probe was 5’-FAM and 3’-MGB-labeled, and its nucleotide sequence was 5’-CACTCCCTCTCTGCGCGCTCG.

2.5. *In vitro* Transduction and Neutralization Assay

Wells of 96-well plates were seeded with 8E4 cells each. The next day, medium was aspirated before gently adding 50 µl of fresh culture medium containing 0 to 900 µg/ml (100 µg/ml increments, 10 different concentrations in total) IVIG (Sinopharm Wuhan Plasma-derived Biotherapies). After a 30 min incubation at 37°C, 50 µl of fresh culture medium containing one of the AAV capsid variants at MOI 10,000 vg/cell was added before returning the plates to the incubator. Three replicates were made for each capsid variant / IVIG amount combination. Flow cytometry was performed 72 hours later. After removing medium, wells were washed with 40 µl PBS. After removing PBS, cells were detached from wells using 20 µl of Trypsin-EDTA. After complete detachment, cells were mixed with 150 µl of fresh medium before flow detection was performed on a Cytoflex S (Beckman Coulter). All *in vitro* experiments used cell culture medium supplemented with 10% fetal bovine serum. DMEM was used for A549, HepG2, and HuH-7 cells; DMEM F12 was used for ARPE-19 cells; McCoy’s 5A was used for SKOV-3 cells; RPMI 1640 was used for BxPC-3 cells.

2.6. Animals

For selection in NHPs, two healthy animals (*Macaca fascicularis*) were used in each of the two rounds, first male and female, then male only, 2 to 3 years old, weighing approximately 4 kg each. Selection in mice: three healthy 9- to 10-week-old male C57BL/6J mice weighing 25 to 27 g each were used. Capsid variant evaluation: a total of 35 healthy animals (7 for each of the 5 variants), 4- to 6-week-old female C57BL6 mice weighing 12 to 18 g each, were used. Monkeys were provided by Pharmalegacy (Shanghai); mice for selection were provided by the Suzhou branch of the Shanghai Institute of Materia Medica (SUSIMM, Suzhou), and mice for capsid variant evaluation were purchased from Beijing Vital River Laboratory Animal Technology (Beijing). Mice were housed in an SPF environment with *ad libitum* access to food and water,and were acclimated for one week before the experiments.

No exclusion or inclusion criteria were used. All animals used in experiments were included in the analyses. Animals were allocated randomly, and operators were blinded to the identity of the injected capsid variant.

All animal experimental procedures were approved by the Institutional Animal Care and Use Committee (IACUC #20240111), ViewGene Biotech Co. Ltd (Suzhou, Jiangsu Province, China), and were carried out in accordance with the recommendations in the Guide for the Care and Use of Laboratory Animals, adhering to the ARVO Statement for the Use of Animals in Ophthalmic and Vision Research.

2.7. Cell Lines

Provenance details of cell lines used in this study were as follows:

AAV-293: NCACC (Shanghai), cat. number GNHu13.

A549: NCACC (Shanghai), cat. number SCSP-503.

HepG2: NCACC (Shanghai), cat. number SCSP-510.

BXPC-3: NCACC (Shanghai), cat. number SCSP-529.

ARPE-19: Procell Life Science & Technology (Wuhan), cat. number CL-0026.

HuH-7: Procell Life Science & Technology (Wuhan), cat. number CL-0120.

SKOV-3: ATCC, cat. number HTB-77.

2.8. Intravitreal rAAV Injections

Intravitreal injections of AAV capsid libraries into NHPs were performed by Pharmalegacy (Shanghai). Two animals were used in each of the two rounds and injected into a single eye. In the first round, injection volume was 50 µl and capsid library titer was 1.44E13 vg/ml. In the second round, injection volume was 100 µl and capsid library titer was 6.07E13 vg/ml.

Intravitreal injections of the AAV capsid library into mice were performed by SUSIMM (Suzhou) using three animals, with both eyes of each animal injected with 1 µl of the AAV preparation, which had a titer of 4.50E13 vg/ml.

The following describes intravitreal injections of rAAV preparations for capsid variant evaluation. Mice were anesthetized by intraperitoneal injection of 1.25% Avertin (Nanjing Aibei Biotechnology, 0.33-0.39 ml / 20 g animal weight). One microliter (7.22E9 vg) of rAAV particles was intravitreally injected using a 30-gauge beveled needle. The injection was performed freehand under a surgical microscope (66 Suzhou Vision-Tech). Both eyes were injected. Seven animals were used for each sample.

2.9. Retinal Harvesting

For capsid library selection in NHP, whole retinas were harvested by Pharmalegacy (Shanghai) 14 days after intravitreal injection.

For capsid library selection in mice, whole retinas were harvested by SUSIMM (Suzhou) 7 days after intravitreal injection.

For capsid variant evaluation, 3 weeks after intravitreal injection, mice were anesthetized by intraperitoneal injection of 1.25% Avertin (Nanjing Aibei Biotechnology, 0.33-0.39 ml / 20 g animal weight). Five minutes later, mice were euthanized by cervical dislocation. Eyes were enucleated by pulling apart the eyelids, placing a curved forceps under the eyeball, closing the forceps and gripping the connective tissue and optic nerve, being careful to avoid squeezing the eyeball, and gently pulling the eyeball from the orbit.

2.10. Retinal Flat Mounts

Eyes were fixed with 4% PFA (paraformaldehyde solution, Solarbio, Beijing) at 4°C for 1 hour, then washed

twice with PBS. An 18G needle was used to make a small hole in the posterior of the limbus. Micro-scissors were then used to cut around the circumference of the limbus. The cornea, iris, lens, and sclera were removed using forceps. The vitreous gel was extracted by gently squeezing it out with the help of micro-forceps. Two pairs of micro-forceps were used to go around the edges to separate the retina from the eyecup and then gently squeeze the retina out. The optic nerve head area was gently cut with micro-forceps. The neuroretina was carefully peeled off the RPE/choroid and immersed in PBS buffer. Flat mounts were transferred to glass slides and mounted with the RGC layer facing upward using PBS. Images for assessment of GFP densities were acquired by fluorescence microscopy (Olympus IX70) and captured with a CCD camera (RETIGA 1300I) and associated software (Q Capture X64 software).

2.11. Retinal Cryosections

Enucleated eyes were fixed in 4% PFA/PBS for 4 hours at 4°C, followed by overnight incubation in 30% sucrose/PBS and embedded in optimal cutting temperature (OCT) reagent (Solarbio, Beijing) before being frozen. A Leica CM cryostat was used to make 15-20 µm sections, which were collected on slides coated with polylysine and stored at -20°C. Retinal sections were stained with DAPI solution (Sangon Biotech, Shanghai, 5 mg/L) for 10-15 minutes in the dark and washed twice with 0.1% Triton-X-100 (Sigma-Aldrich) in PBS. Slides were scanned, and images were taken under an inverted fluorescence microscope (Olympus IX70).

2.12. Data Visualization

Protein sequence features were computed using Parent-map [17]. The three-dimensional capsid structure model was rendered by PyMOL [18] using data (PDB ID 7KP3) obtained from VIPERdb [19].

2.13. Sequence Deposition

Nucleotide sequence of the novel capsid variant PT1 was deposited in GenBank under accession number PQ252346.

3. RESULTS

3.1. Capsid Variant Development

An AAV5-based capsid library was developed as previously described [11, 12] and subjected to two rounds of *in vivo* selection in cynomolgus macaque retina *via* intravitreal injection. An enriched capsid variant with a total of eight amino acid substitutions in three variable regions was identified: TEN to EKH at 376-378 in VR-III, S518K in VR-VI, and ND to SE at 694-695, Q697T, and T706A in VR-IX (Fig. **1**). A new capsid library was then designed and constructed based on that variant, with mutations in variable regions IV and VIII. The new library was subjected to a single round of *in vivo* selection in murine retina *via* intravitreal injection. Enriched mutation N443A (VR-IV), as well as an enriched motif consisting of mutations N573A, SST to NAS at 575-577, and AT to TA at 581-582 (VR-VIII), were identified. Finally, as we had previously observed in swapping experiments that the transduction efficiency of AAV5-derived capsid variants can be significantly increased by replacing their VP1-unique region by that of AAV8 (unpublished), it was decided to apply this sequence swap to our new variant. In summary, the final capsid variant, referred to hereafter as PT1, can be defined, as illustrated in Fig. (**1**), as having an AAV8 VP1-unique region, with the rest of the sequence deriving from AAV5, with a total of 15 amino acid substitutions in five different variable regions.

3.2. Recombinant AAV Preparations

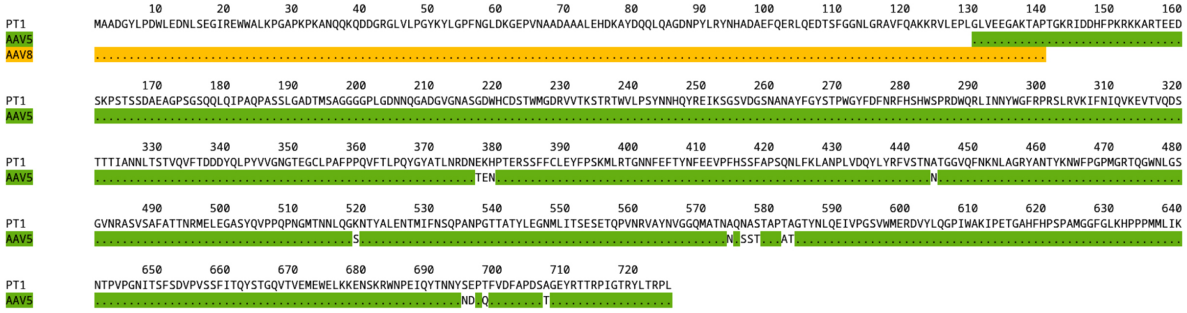
Four capsid variants capable of transducing retina after intravitreal injection were selected as controls to which the novel capsid PT1 was to be compared. Wild-type AAV2, used in the first approved retinal gene therapy Luxturna (although administered subretinally) as well as in most early clinical trials of intravitreally injected gene therapies, was an obvious first choice. Two other AAV2-derived capsids with improved properties, the rationally designed quintuple mutant AAV2(quadY-F+T-V) [10], hereafter designated as quadYFTV, and the evolved capsid 7m8, harboring a 10-amino-acid insertion in variable region VIII [7], were chosen as well. Finally, the recently announced AAV5-derived LSV1 [20] seemed to be particularly relevant as being a capsid variant quite similar to PT1 but with a different set of mutations.

A recombinant AAV genome encoding GFP under a CMV promoter was packaged with the five capsid variants (PT1 and the four controls). Two preparations, 7m8 and quadYFTV, had high endotoxin levels and were subjected to an endotoxin removal step [16]. As expected, the AAV5-derived variants LSV1 and PT1 had higher yields (2.8E13 and 2.6E13 vg, respectively) than the AAV2-derived capsids (7.2E12 to 1.5E13 vg). In order to reach the same working titer for all preparations, four of them were diluted to the same titer as AAV2, which was the lowest at 7.22E12 vg/ml.

3.3. *In vitro* Transduction

Transduction efficiency of PT1 was compared to that of the four control capsids AAV2, quadYFTV, 7m8 and LSV1 in the relevant human retinal pigment epithelial cell line ARPE-19 [21], and quantified using flow cytometry. As shown in Fig. (**2**) (left), all five capsids show similar transduction, from 79.8% GFP-positive cells for AAV2 to 91.6% for LSV1, with PT1 being in the middle at 86.8%.

In addition, transduction efficiencies of PT1 and AAV2 were compared in five additional human-derived cell lines (chosen because they happened to be readily available): A549, HepG2, HuH-7, SKOV-3 and BxPC-3 (Fig. **2** right). AAV2 appears to show broad cell tropism, with over 40% transduction in all six cell lines, lowest at 43.1% in A549 and highest in the two liver-derived cell lines HuH-7 (90.2%) and HepG2 (87.8%). In contrast, PT1 shows a strong preference for ARPE-19 cells with 86.8% transduction, significantly lower transduction in HuH-7 (62.6%) and much lower (below 40%) in all four other cell lines.



Variant region	Parent / feature	Parent region	Variant sequence	Parent sequence	Variable region	Selected in
1-140	AAV8	1-140				In vitro
130-376	AAV5	129-375				
377-379	substitution	376-378	EKH	TEN	III	NHP
380-443	AAV5	379-442				
444	substitution	443	A	N	IV	Mouse
445-518	AAV5	444-517				
519	substitution	518	K	S	VI	NHP
520-573	AAV5	519-572				
574	substitution	573	A	N	VIII	Mouse
575	AAV5	574			VIII	
576-578	substitution	575-577	NAS	SST	VIII	Mouse
579-581	AAV5	578-580			VIII	
582-583	substitution	581-582	TA	AT	VIII	Mouse
584-694	AAV5	583-693				
695-696	substitution	694-695	SE	ND	IX	NHP
697	AAV5	696			IX	
698	substitution	697	T	Q	IX	NHP
699-706	AAV5	698-705			IX	
707	substitution	706	A	T	IX	NHP
708-725	AAV5	707-724				

Fig. (1). Sequence features of capsid variant PT1. Top: amino acid sequence of PT1 capsid VP1 protein compared with parent capsids AAV8 (gold) and AAV5 (green). Dots indicate identity. Parental sequences are only shown when they differ from that of PT1. Bottom left: Three-dimensional model of AAV5 capsid showing the surface substitutions of PT1 color-coded according to their region (red: VR-III, green: VR-IV, blue: VR-VI, yellow: VR-VIII, magenta: VR-IX). Bottom right: detailed description of PT1 capsid VP1 sequence. Substitutions are color-coded in the same way as the model on the left.

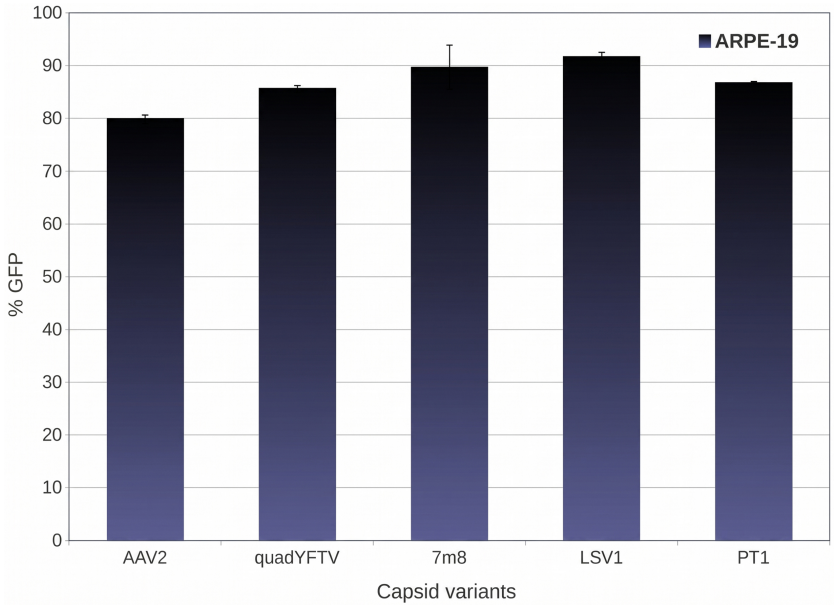


Fig. 2 contd.....

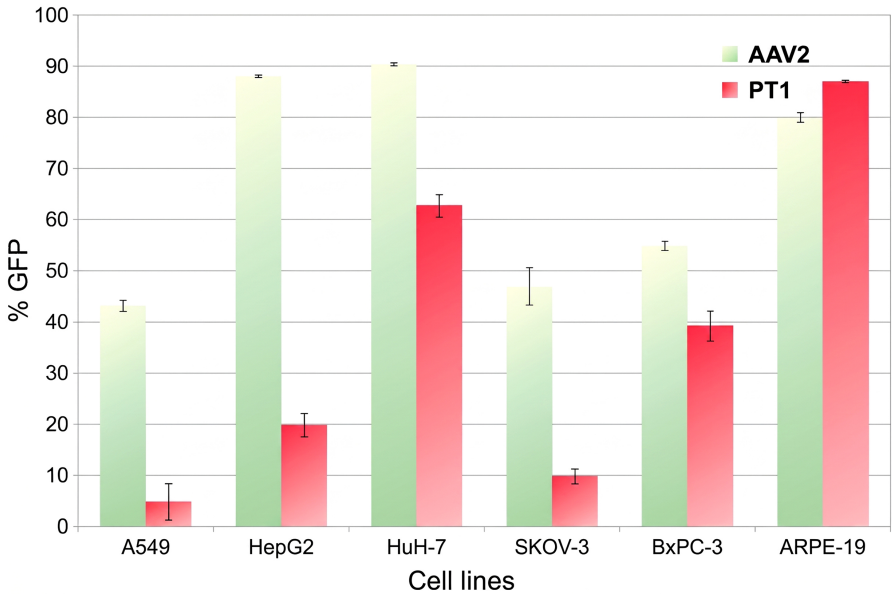


Fig. (2). *In vitro* transduction comparisons. Left: transduction efficiencies (percentage of GFP-positive cells) in the ARPE-19 cell line of PT1 compared with that of four control capsids. Right: comparison of transduction efficiencies of AAV2 and PT1 in six different cell lines. Error bars show standard deviation.

3.4. Immune Evasion

In order to determine to what extent PT1 can evade preexisting NABs compared to the four control capsids, ARPE-19 cells preincubated with increasing amounts of commercial human intravenous immunoglobulin (IVIG) of Chinese origin were infected with GFP-encoding rAAV preparations. Three days later, the prevalence of GFP-expressing cells was quantified by flow cytometry. As shown in Fig. (3), while all four controls saw a 90% or more decrease in transduction at 100 µg/ml IVIG, 900 µg/ml IVIG was necessary to achieve the same level of neutralization with PT1. The IVIG concentration required to reach 50% neutralization was 14, 15, 21, 31, and 286 µg/ml, respectively, for AAV2, quadYFTV, 7m8, LSV1, and PT1.

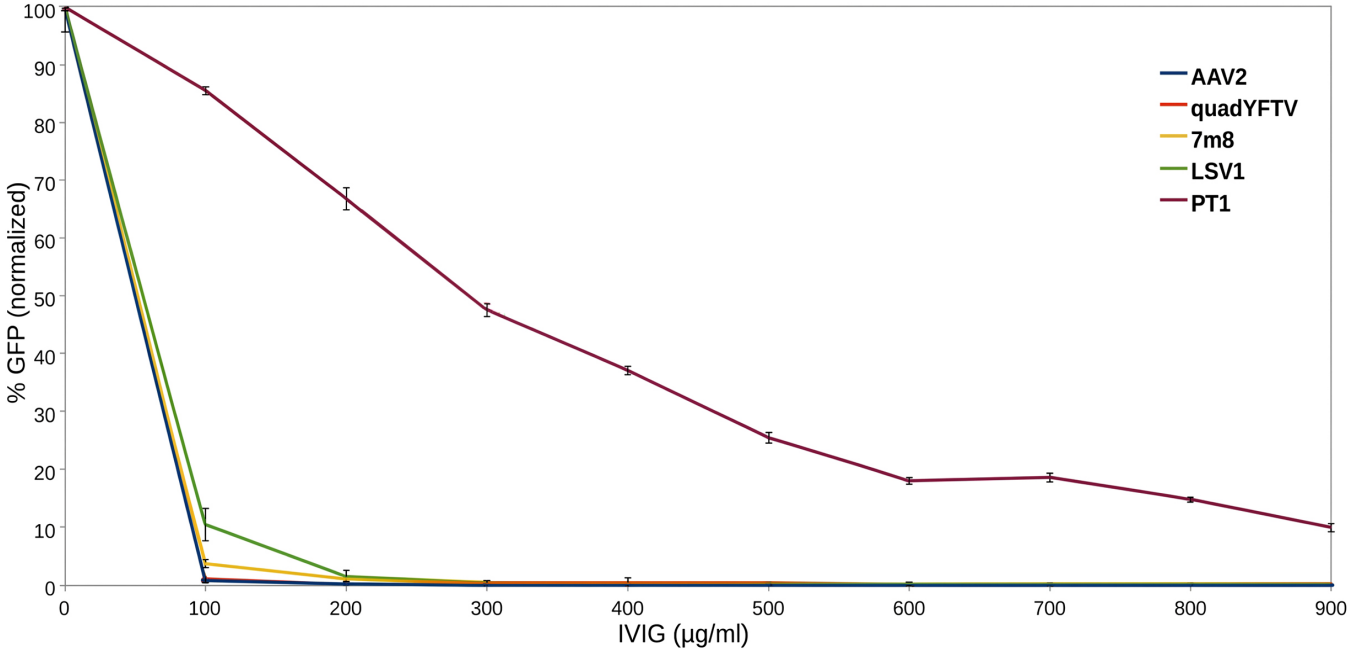


Fig. 3 contd.....

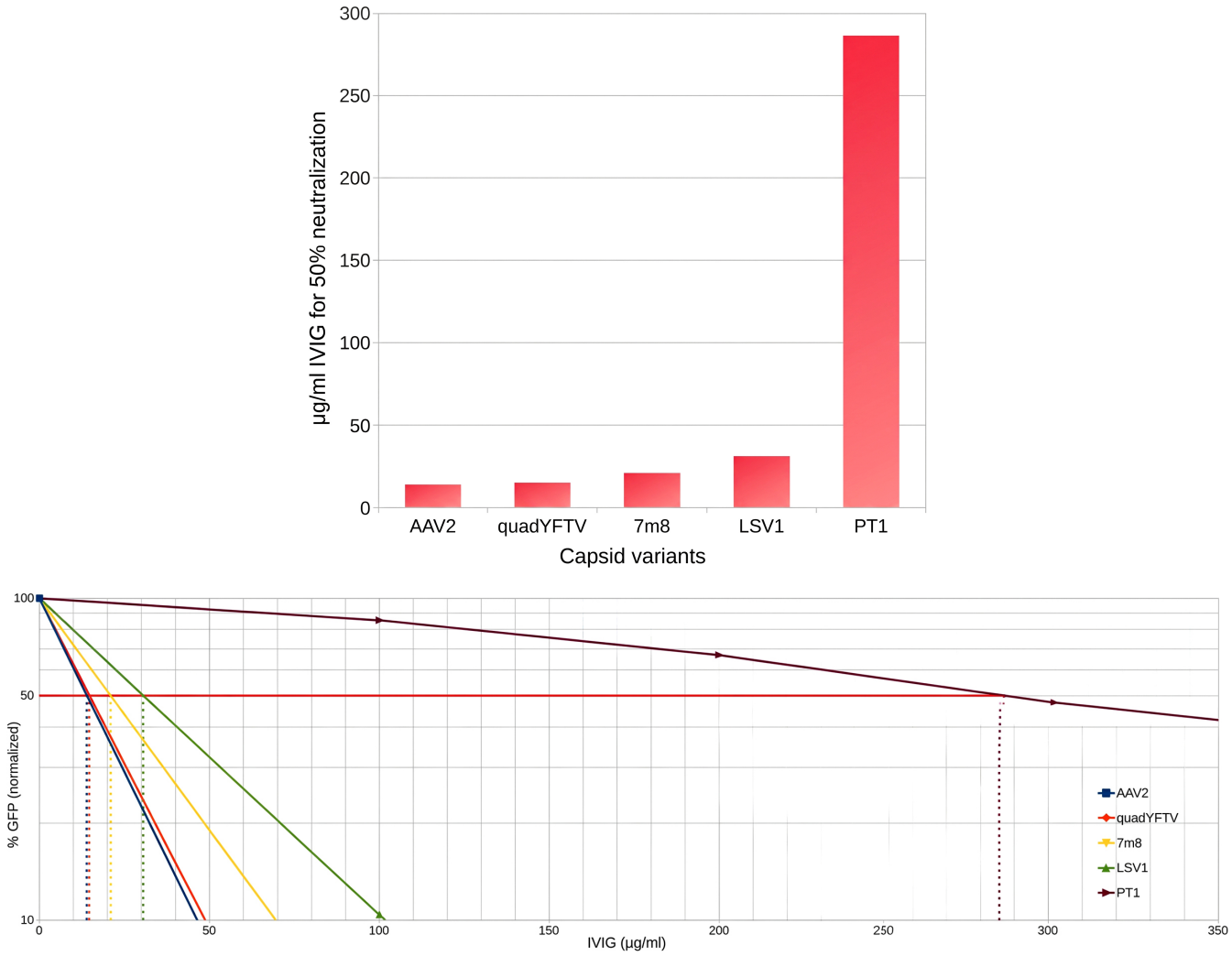


Fig. (3). *In vitro* neutralization assays of PT1 and four control capsids in ARPE-19 cells. Top left: comparison of transduction neutralization by increasing amounts of IVIG of PT1 and four control capsids. Error bars represent standard deviation. Bottom: zoom of relevant area of above chart with Y-axis converted to logarithmic scale for easier visualization of the IVIG concentrations at which 50% neutralization is achieved. Top right: comparison of neutralization scores (IVIG concentration needed for 50% decrease in transduction) for PT1 and the four control capsids.

To assess whether PT1 would display similar immune-evading properties under different experimental conditions, the neutralization assay was repeated using five additional human cell lines but with AAV2 only as a control (Fig. **4**). The same pattern was observed in all cases, with PT1 substantially outperforming AAV2 in its ability to evade neutralization. However, some variation in neutralization scores (IVIG concentration for 50% neutralization) was observed, with a ratio of 3 between the highest and lowest scores for AAV2 and 2.55 for PT1. Ratios between PT1 and AAV2 scores varied as well, from 4.9 in HuH-7 cells to 20.4 in ARPE-19 cells.

3.5. *In vivo* Evaluation

Each of the five rAAV preparations was injected intravitreally into both eyes of seven mice, 1 µl (7.22E9 vg) each. Eyes were harvested three weeks later. For each animal, one eye was processed into a flat mount in order to observe overall retinal transduction, while the other eye was processed as frozen sections to evaluate the biodistribution of GFP expression across the various retinal layers.

Retinal flat mount images are shown in Fig. (**5**). AAV2 and its two derivatives, quadYFTV and 7m8, showed the largest transduced areas, with 7m8 performing best. Very little GFP expression was observed with LSV1. While other variants showed mostly a continuous central area of GFP expression, in PT1 the expression was localized in smaller discrete areas distributed over the whole retina.

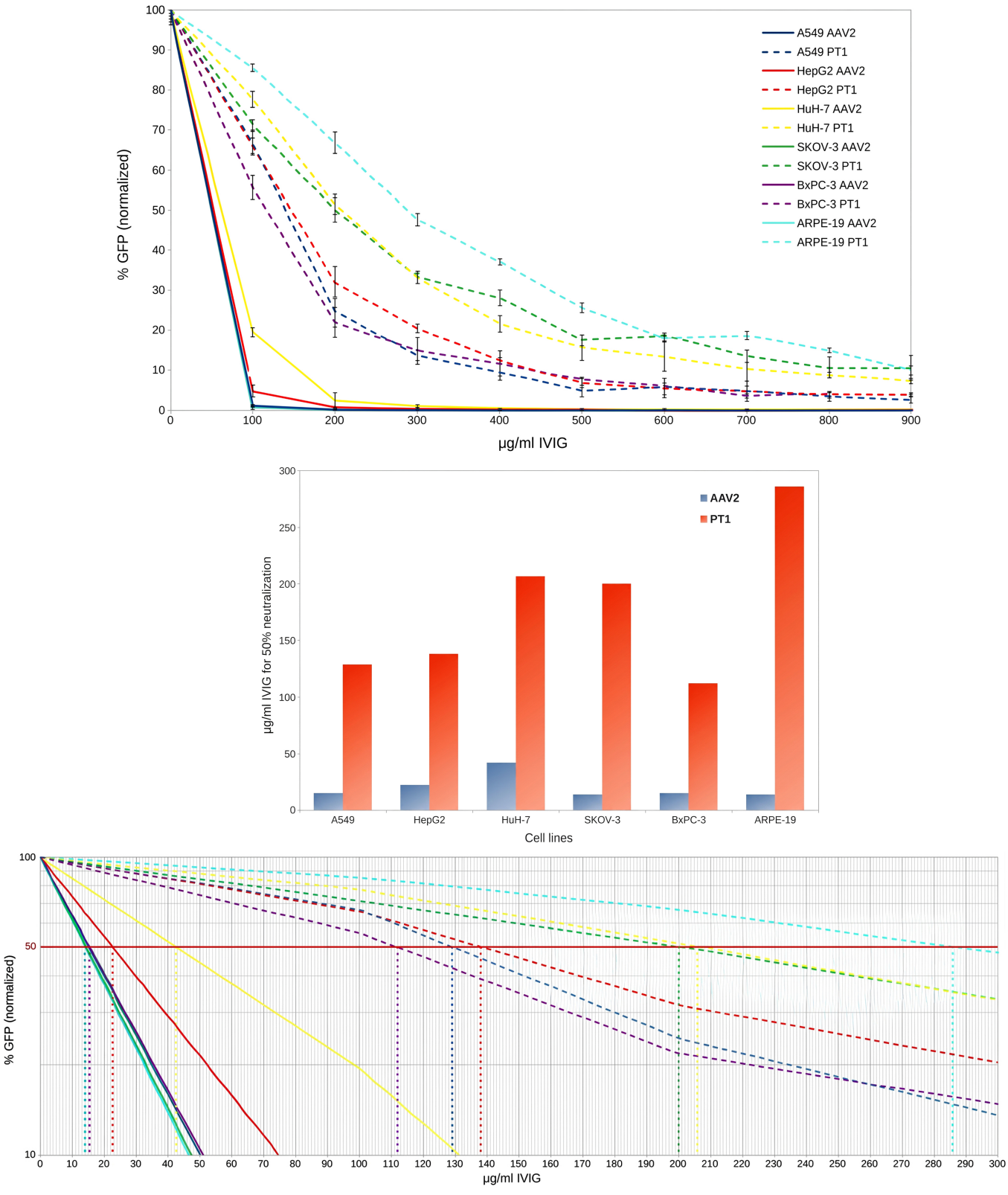


Fig. (4). *In vitro* neutralization assays of PT1 and AAV2 capsids in six different cell lines. Top left: neutralization by IVIG of PT1 and AAV2 in six cell lines. Bottom: zoom on relevant area with Y-axis converted to logarithmic scale, showing IVIG concentrations at which transduction is decreased by 50%. Top right: comparison of neutralization scores between PT1 and AAV2 in six cell lines.

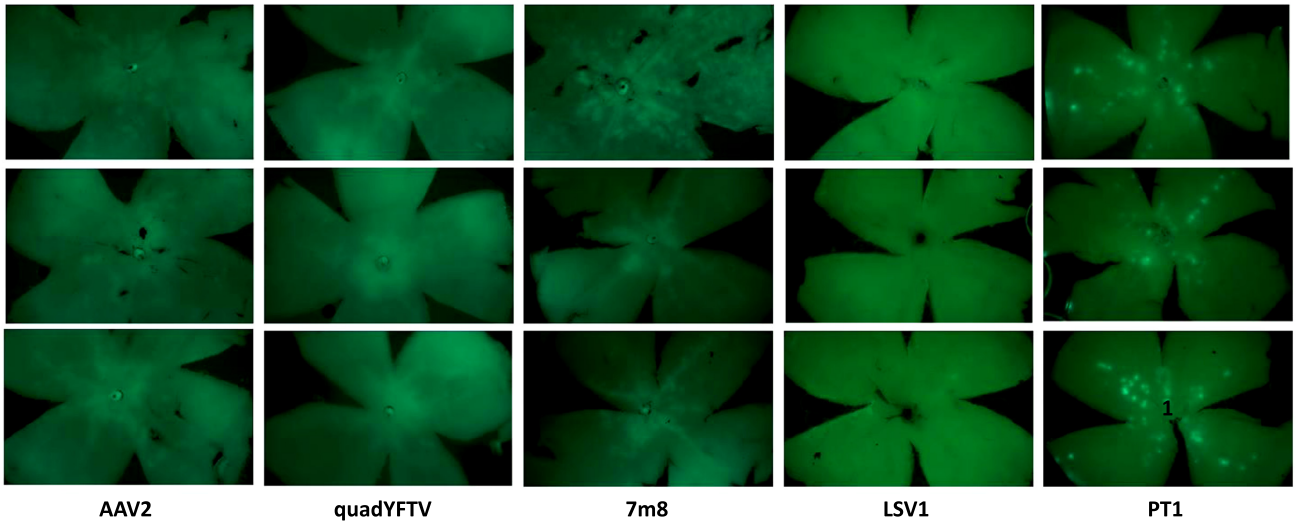


Fig. (5). Retinal flat mounts. Fluorescence microscopy images of three representative retinal flat mounts are shown for each variant (all images are available in the repository referenced in the Data availability section). From left to right: AAV2, quadYFTV, 7m8, LSV1, PT1. For LSV1 and PT1, exposure time was increased to make GFP expression more visible.

Retinal cryosections are shown in Fig. (**6**). Again, the three AAV2-related capsid variants had broader transduction areas, while LSV1 had the lowest. The four control variants had a quite similar transduction pattern, with GFP expression concentrated mostly in the ganglion cell layer (GCL) and the inner nuclear layer (INL). In stark contrast, PT1 seemed to specifically target elongated cells spanning the entire retina width. These observations suggest that while AAV2, quadYFTV, 7m8, and LSV1 mostly transduce neuronal cells, PT1 transduces mostly Müller glial cells.

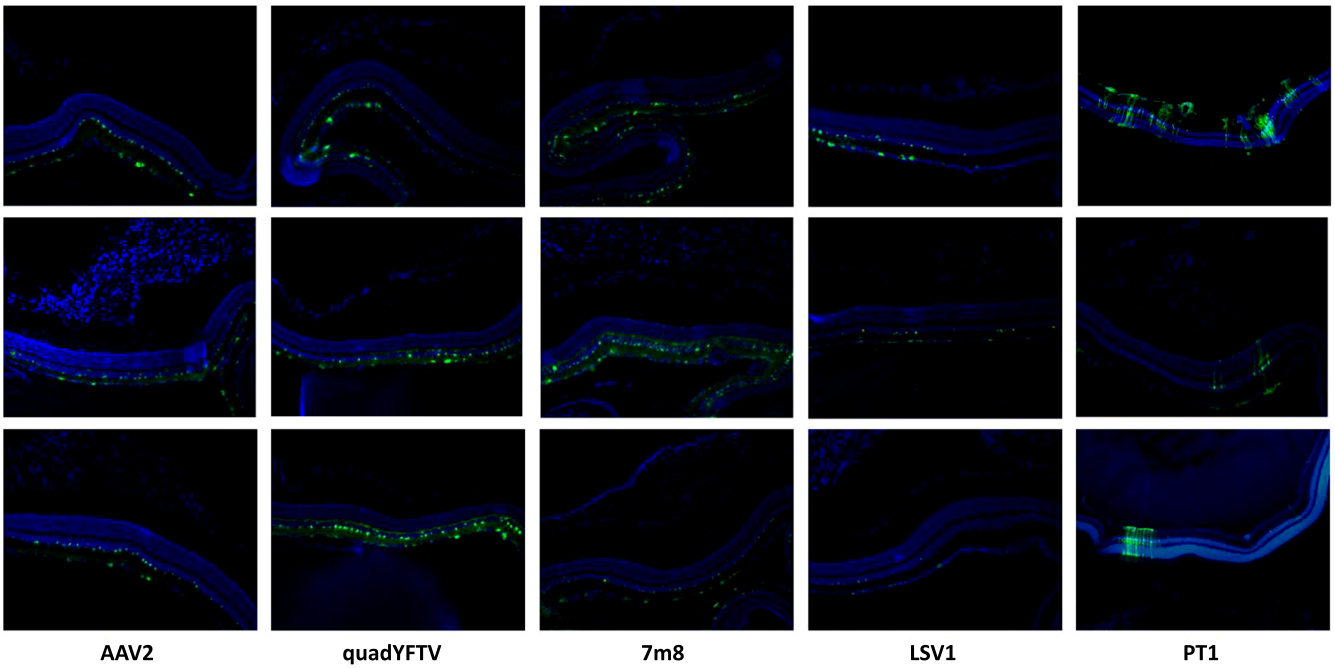


Fig. (6). Retinal cryosections. Fluorescence microscopy images of three representative retinal cryosections are shown for each variant (all images are available in the repository referenced in the Data availability section). From left to right: AAV2, quadYFTV, 7m8, LSV1, PT1.

4. DISCUSSION

An AAV5-based multiple loop swap capsid library was developed and subjected to two rounds of *in vivo* selection in non-human primates (NHP). The AAV5 capsid was chosen as the library backbone because it had not been widely used for capsid libraries; it is the most divergent among human AAV capsid serotypes [22, 23]; it has excellent thermal stability [24]; and it shows low prevalence of NABs among human populations [25]. As the retinal gene therapy literature is mostly dominated by AAV2-derived capsids, it was interesting to explore an alternative such as AAV5, which could offer potential advantages both in terms of manufacturability (higher expression yield and stability) and patient safety and eligibility (more favorable immune profile).

The main purpose of the AAV5-derived capsid library was not to develop a retinal capsid, but rather to target organs such as liver, heart, or kidneys through intravenous injection (not addressed in this report). It was decided to also inject intravitreally into the same animals to maximize the amount of data that could be obtained per animal. This was an exploratory approach undertaken without a strong prior basis for expecting success, since at the time, only AAV2-derived capsids were known to efficiently transduce retina after intravitreal injection. Nevertheless, an enriched variant was identified in retinal tissue, with a total of eight amino acid substitutions in the three variable regions VR-III, VR-VI, and VR-IX. As the VR-IV and VR-VIII regions were not mutated, while they are the two regions with the highest spikes on the AAV5 capsid surface (Fig. **1**), we decided to further evolve our variant by creating a capsid library based on it with mutations in those two regions, and subject the library to *in vivo* selection. Having no longer access to NHPs, mice were used instead. After a single round of selection in retinal tissue after intravitreal injection, seven additional amino acid substitutions were found to be strongly selected for, one in VR-IV and six in VR-VIII. The novel PT1 capsid variant combines the 15 mutations selected in NHP (eight mutations) and mice (seven mutations) with an additional swap of the VP1 unique region with that of AAV8 to increase transduction efficiency (Fig. **1**). PT1 was compared to relevant capsid variants known to transduce retina after intravitreal injection, including AAV2 and two of its derivatives, 7m8 and quadYFTV, as well as the AAV5-derived LSV1.

Having a large number of mutations did not appear to interfere with capsid assembly, as the production yield of PT1 was similar to that of LSV1 and higher than that of the AAV2-derived variants.

The sample size (number of animals used) during directed evolution was constrained by financial limitations, although at least two animals were used in each step to limit possible effects of inter-individual variation. It is quite possible that using more animals or additional rounds of selection would have helped identify different sets of mutations and different capsid properties. On the other hand, accounting for inter-individual variation was much more important during *in vivo* evaluation, which is why a larger sample size of seven animals per capsid was used, conforming with common practice in the field, and justified *post-hoc* by actually observing little such variation.

The ability to transduce retinal tissue was first assessed *in vitro* using ARPE-19 cells, derived from human retinal pigmented epithelium. All five capsid variants showed similarly efficient transduction. When comparing transduction of various human-derived cell lines between PT1 and AAV2, PT1 showed a strong preference for the retinal cells ARPE-19, while AAV2 showed more versatility and a slight preference for liver-derived cells (Fig. **2**).

The most remarkable finding about PT1 is its striking ability to evade preexisting NABs (Figs. **3** and **4**) under our experimental conditions. This is particularly relevant in the context of intravitreal delivery of gene therapies, as the vitreous is not as immune-privileged as the subretinal space [4], and the availability of better immune-evading capsids will allow larger patient populations to be treated. This notable property of PT1 is not merely due to PT1 deriving from AAV5, since AAV5-derived LSV1 only performs slightly better than the three AAV2-derived capsids, far behind PT1. The number of surface mutations (15 and 9 for PT1 and LSV1, respectively) cannot be the main reason either. An important difference between the two capsids is that all nine LSV1 mutations are confined within a very short 12-amino-acid-long region in VR-VIII, while the 15 PT1 mutations are spread over a huge, 331-amino-acid-long region and are present within five different variable regions (VR-III, VR-IV, VR-VI, VR-VIII and VR-IX), altering the capsid surface on a much larger scale. AAV5 capsid epitopes were previously described in structural studies involving four different monoclonal antibodies complexed with the AAV5 capsid [26-28]. Their overlap with LSV1 and PT1 mutations is shown in Table **1**. Only two out of the nine LSV1 mutations correspond to a contact position, both with the same antibody HL2476. On the other hand, seven of the 15 PT1 mutations correspond to contact positions involving all four antibodies ADK5a (four positions), ADK5b (three positions), HL2476 (three positions) and 3C5 (one position). It should be noted that these seven positions only represent a fraction of the footprints formed by the four reported antibodies. In particular, epitopes exist in regions VR-I, VR-II, VR-V, VR-VII, and the HI loop, which are all wild-type in PT1, suggesting that even more radical immune evasion might be possible by introducing mutations in these regions. It remains to be seen, however, whether this could be achieved without compromising the efficiency of capsid assembly or the ability to transduce retinal cells.

In vivo evaluation in mice showed that overall, 7m8 was the most effective at transducing the retina, while PT1 was superior to LSV1 (Figs. **5** and **6**). However, while all four controls transduced primarily cells located in the retinal layers closest to the vitreous (GCL and INL), PT1 had a strikingly distinct transduction pattern, targeting elongated cells stretching radially across the thickness of the retina, most likely Müller glial cells, in a focal manner.

Table 1. Mutated amino acid positions in LSV1 or PT1 that have previously been described as AAV5 epitopes. Numbers indicate amino acid positions using AAV5 VP1 numbering (LSV1 and PT1 numbering are different because their VP1 unique regions were swapped with those of AAV2 and AAV8 respectively, which are of different length). ADK5a, ADK5b, HL2476 and 3C5 are monoclonal antibodies whose interactions with the AAV5 capsid were previously described. The plus sign indicates a contact position between the antibody and the capsid. Mutations in LSV1 and PT1 relative to AAV5 are shown (positions are wild type if blank).

Position	ADK5a [28]	ADK5b [28]	HL2476 [27]	3C5 [26]	LSV1	PT1
377	+					E to K
378	+					N to H
443		+	+			N to A
576			+			S to A
577			+		T to G	T to S
578			+		T to D	
697	+	+				Q to T
706	+	+		+		T to A

This property makes PT1 quite uncommon among intravitreal retinal capsids, which typically have broad retinal tropism. Actually, another capsid variant has previously been reported to target Müller glial cells after intravitreal injection: ShH10, derived from AAV6 [29]. Its authors report 62% better efficiency at infecting Müller cells for ShH10 relative to AAV2, apparently lower than PT1 relative to AAV2 in our observations (Fig. **6**). It would therefore be interesting to perform a side-by-side comparison of PT1 and ShH10 to determine which capsid outperforms the other in terms of transduction efficiency and Müller cell specificity. The ability to target Müller glial cells is of great interest for retinal gene therapy, as Müller cells provide functional, metabolic, and structural support to retinal neurons and are resistant to degenerative diseases [30]. Furthermore, it was shown recently that Müller glia-mediated retinal regeneration, which is normally suppressed in mammals, can be induced using gene therapy approaches [31, 32].

The present report is only a preliminary exploration of PT1 properties. An extensive evaluation will be needed to confirm our initial findings and assess PT1's potential as a possible gene therapy vector. Below are listed some of the limitations of the present work and suggested strategies for future research.

For proper comparison, it is crucial that all variants be prepared in the same manner and have identical purity levels, full/empty capsid ratios, and titers. Here, two variants (7m8 and quadYFTV) had high endotoxin levels, likely due to different plasmid purification kits being used to prepare the rep-cap plasmids used during transfection, and had to be subjected to an endotoxin-removal purification step. Full/empty capsid ratios were not determined, although they were expected to be relatively similar as a result of purifying the viral preparations using ultracentrifugation. Titers were only determined using qPCR (but with probes, giving more accurate results than with the SYBR green method), while a second method such as ddPCR would have given more confidence in their values. However, variations in purity or inaccuracies in titers are unlikely to change the key findings about PT1, which are its remarkable immune evasion properties and apparent specificity for Müller glial cells. Higher confidence about titers would allow to more accurate comparison of overall retinal transduction levels between variants.

Evasion of preexisting NABs was only evaluated *in vitro* using a single IVIG supply, which, although pooled from thousands of individuals, was of limited geographical origin (China). Although results would not be expected to be significantly different using IVIG sourced from other geographical locations, doing so would represent an important confirmation. Therefore, future studies should include multiple IVIG samples representing diverse human populations, as well as large numbers of individual serum samples. In addition to evasion of preexisting NABs, it would also be useful to compare variants for their immunogenicity by evaluating *in vivo* ocular inflammation as well as the occurrence of triggered NABs after injection.

PT1's apparent Müller glia specificity was inferred solely from morphology and will require more experimental validation. Higher resolution microscopy using appropriate cell-specific staining will allow precise tropism determination. In addition to confirming PT1's preference for Müller glia, it will be interesting to observe how strong its specificity is and what other cell types are also transduced, ideally not just in mice but also in the more clinically relevant NHP. Alternatively, transduction assessment in the various retinal cell types could also be done using iPSC-derived retinal organoids or *ex vivo* human retinal explants.

It would also be worth exploring to what extent PT1 mutations improve penetration of the inner limiting membrane (ILM). It is known that contrary to AAV2, AAV5 does not bind ILM receptors and has very low penetration as a result [33]. Investigating which sets of mutations are responsible for which improvements (ILM penetration, cell transduction, post-entry stability) would help inform further development by engineering additional mutations.

Finally, the choice of control capsids could be improved. The four control capsid variants used here turned out to have very similar properties compared to PT1. Only the AAV2-derived 7m8 should be kept as a gold standard, while wild-type AAV5 should be the background control. The variants with the eight mutations from the selection in NHP and with the seven additional mutations selected in mice would inform which set of mutations affect transduction efficiency, immune evasion, and cell specificity, and whether these effects are species-specific. Comparing PT1 with the latter would also reveal the extent of improvement in transduction efficiency due to the VP1 unique region swap. Lastly, previously described Müller glia-targeting capsid variant ShH10 should be included as a control as well.

5. STUDY LIMITATIONS

Full/empty capsid ratios were not determined, and titers were determined using qPCR only.

Relevant capsid variant ShH10 was not included in side-by-side comparisons.

Müller cell specificity was inferred from morphology alone; no molecular validation was performed.

In vivo experiments did not include dose-response or safety studies and only had a short three-week endpoint with no long-term expression data.

No NAB measurements or ocular inflammation assessments were performed post-injection.

CONCLUSION

The novel AAV capsid variant PT1 shows that AAV5 can be a suitable alternative to AAV2 as a parent capsid for evolving variants for retinal gene therapy *via* intravitreal injection, with advantages including higher production yield and a more favorable immune profile.

Incremental development, with selection of mutations in a limited set of variable regions followed by selection in another set of additional variable regions, combined with a rationally designed swap of the VP1 unique region, allowed the generation of a capsid variant with the desired property of improved retinal transduction after intravitreal injection without impairing the efficiency of capsid assembly.

Thanks to the large number of mutations spread over the capsid surface, with several positions overlapping with known epitopes, the novel capsid variant PT1 has a remarkable ability to evade preexisting NABs under our limited experimental conditions. Another interesting property is PT1's apparent targeting of Müller glial cells, which would be particularly relevant for human gene therapy applications.

Because of limitations due to the limited scope of the current work, stronger claims about PT1 are pending confirmation by further studies. However, the initial findings presented here suggest PT1 or some of its further engineered variants could become useful tools for human retinal gene therapy *via* intravitreal delivery, should our initial findings be confirmed by further experimental evidence.

AUTHORS' CONTRIBUTIONS

The authors confirm their contributions to the paper as follows: D.M.: Study conception and design; Z.C., Y.L., L.Z., X.L., B.Z., Y.T., T.Z., Z.Z. and A.L.: Data collection; Z.C., Y.L., L.Z., J.W., Q.J., D.L. and D.M.: Analysis and interpretation of results; Z.C., Y.L., J.W. and D.M.: Draft manuscript preparation. All authors reviewed the results and approved the final version of the manuscript.

LIST OF ABBREVIATIONS

AAV	=	Adeno-Associated Virus
NABs	=	Neutralizing Antibodies
IACUC	=	Institutional Animal Care and Use Committee
OCT	=	Optimal Cutting Temperature
GCL	=	Ganglion Cell Layer
INL	=	Inner Nuclear Layer
NHP	=	Non-Human Primates
ILM	=	Inner Limiting Membrane

ETHICS APPROVAL AND CONSENT TO PARTICIPATE

All animal experimental procedures were approved by the Institutional Animal Care and Use Committee (IACUC #20240111), ViewGene Biotech Co. Ltd (Suzhou, Jiangsu Province, China).

HUMAN AND ANIMAL RIGHTS

This study adheres to internationally accepted standards for animal research, following the 3Rs principle. The ARRIVE guidelines were employed for reporting experiments involving live animals, promoting ethical research practices.

Experiments on animals were carried out in accordance with the recommendations in the Guide for the Care and Use of Laboratory Animals, adhering to the ARVO Statement for the Use of Animals in Ophthalmic and Vision Research.

CONSENT FOR PUBLICATION

Not applicable.

AVAILABILITY OF DATA AND MATERIALS

Original data presented in this study are openly available in FigShare at https://figshare.com/collections/PT1_AAV_capsid/7461079.

FUNDING

None.

CONFLICT OF INTEREST

The author, Dr. Damien Marsic is on the Editorial Advisory Board of The Open Biotechnology Journal.

ACKNOWLEDGEMENTS

The author Dr. Daru Lu acknowledges the support by National Key R&D Program 2023YFC2705602. The authors would like to thank Lingjie Kong for his continuous support and exemplary leadership. They extend their deep gratitude to Oliver Ju, who made this work possible thanks to his trust and generosity.

REFERENCES

[1] Wang JH, Gessler DJ, Zhan W, Gallagher TL, Gao G. Adeno-associated virus as a delivery vector for gene therapy of human diseases. Signal Transduct Target Ther 2024; 9(1): 78. http://dx.doi.org/10.1038/s41392-024-01780-w PMID: 38565561

[2] Liu F, Li R, Zhu Z, Yang Y, Lu F. Current developments of gene therapy in human diseases. MedComm 2024; 5(9): e645. http://dx.doi.org/10.1002/mco2.645 PMID: 39156766

[3] Gao J, Hussain RM, Weng CY. Voretigene neparvovec in retinal diseases: A review of the current clinical evidence. Clin Ophthalmol 2020; 14: 3855-69. http://dx.doi.org/10.2147/OPTH.S231804 PMID: 33223822

[4] Kotterman MA, Yin L, Strazzeri JM, Flannery JG, Merigan WH, Schaffer DV. Antibody neutralization poses a barrier to intravitreal adeno-associated viral vector gene delivery to non-human primates. Gene Ther 2015; 22(2): 116-26. http://dx.doi.org/10.1038/gt.2014.115 PMID: 25503696

[5] Zolotukhin S, Vandenberghe LH. AAV capsid design: A Goldilocks challenge. Trends Mol Med 2022; 28(3): 183-93. http://dx.doi.org/10.1016/j.molmed.2022.01.003 PMID: 35093287

[6] Srivastava A. Rationale and strategies for the development of safe and effective optimized AAV vectors for human gene therapy. Mol Ther Nucleic Acids 2023; 32: 949-59. http://dx.doi.org/10.1016/j.omtn.2023.05.014 PMID: 37293185

[7] Dalkara D, Byrne LC, Klimczak RR, *et al*. *In vivo*-directed evolution of a new adeno-associated virus for therapeutic outer retinal gene delivery from the vitreous. Sci Transl Med 2013; 5(189): 189ra76. http://dx.doi.org/10.1126/scitranslmed.3005708 PMID: 23761039

[8] Pavlou M, Schön C, Occelli LM, *et al*. Novel AAV capsids for intravitreal gene therapy of photoreceptor disorders. EMBO Mol Med 2021; 13(4): EMMM202013392. http://dx.doi.org/10.15252/emmm.202013392 PMID: 33616280

[9] Kellish PC, Marsic D, Crosson SM, *et al*. Intravitreal injection of a rationally designed AAV capsid library in non-human primate identifies variants with enhanced retinal transduction and neutralizing antibody evasion. Mol Ther 2023; 31(12): 3441-56. http://dx.doi.org/10.1016/j.ymthe.2023.10.001 PMID: 37814449

[10] Kay CN, Ryals RC, Aslanidi GV, *et al*. Targeting photoreceptors *via* intravitreal delivery using novel, capsid-mutated AAV vectors. PLoS One 2013; 8(4): e62097. http://dx.doi.org/10.1371/journal.pone.0062097 PMID: 23637972

[11] Marsic D, Govindasamy L, Currlin S, *et al*. Vector design Tour de Force: Integrating combinatorial and rational approaches to derive novel adeno-associated virus variants. Mol Ther 2014; 22(11): 1900-9. http://dx.doi.org/10.1038/mt.2014.139 PMID: 25048217

[12] Biswas M, Marsic D, Li N, *et al*. Engineering and *in vitro* selection of a novel AAV3B variant with high hepatocyte tropism and reduced seroreactivity. Mol Ther Methods Clin Dev 2020; 19: 347-61. http://dx.doi.org/10.1016/j.omtm.2020.09.019 PMID: 33145371

[13] Keravala A, CEPEDA D, Gasmi M. Variant AAV capsids for intravitreal delivery. US11510950B2, 2021. Available from: https://patents.google.com/patent/US11510950B2/en

[14] Crosson SM, Dib P, Smith JK, Zolotukhin S. Helper-free production of laboratory grade AAV and purification by iodixanol density gradient centrifugation. Mol Ther Methods Clin Dev 2018; 10: 1-7. http://dx.doi.org/10.1016/j.omtm.2018.05.001 PMID: 30073177

[15] Gray J T, Zolotukhin S. Design and construction of functional AAV vectors. In: Snyder R, Moullier P, Eds. Adeno-Associated Virus. Humana Press 2012; 807: pp. : 25-46. http://dx.doi.org/10.1007/978-1-61779-370-7_2

[16] Kondratova L, Kondratov O, Ragheb R, Zolotukhin S. Removal of endotoxin from rAAV samples using a simple detergent-based protocol. Mol Ther Methods Clin Dev 2019; 15: 112-9. http://dx.doi.org/10.1016/j.omtm.2019.08.013 PMID: 31649960

[17] Marsic D. Parent-map: Analysis of parental contributions to evolved or engineered protein or DNA sequences. J Open Source Softw 2021; 6(57): 2864. http://dx.doi.org/10.21105/joss.02864

[18] PyMOL. 2026. Available from: http://www.pymol.org/pymol

[19] Montiel-Garcia D, Santoyo-Rivera N, Ho P, *et al*. VIPERdb v3.0: A structure-based data analytics platform for viral capsids. Nucleic Acids Res 2021; 49(D1): D809-16. http://dx.doi.org/10.1093/nar/gkaa1096 PMID: 33313778

[20] Baker C K, Bennett A, Belbellaa B, *et al*. Novel capsid LSV1 has a unique 3D structure at the loop substitution area-confers superior retinal transduction from intravitreal injection. Mol Ther 2022; 30: 575.

[21] Dunn KC, Aotaki-Keen AE, Putkey FR, Hjelmeland LM. ARPE-19, a human retinal pigment epithelial cell line with differentiated properties. Exp Eye Res 1996; 62(2): 155-70. http://dx.doi.org/10.1006/exer.1996.0020 PMID: 8698076

[22] Chiorini JA, Kim F, Yang L, Kotin RM. Cloning and characterization of adeno-associated virus type 5. J Virol 1999; 73(2): 1309-19. http://dx.doi.org/10.1128/JVI.73.2.1309-1319.1999 PMID: 9882336

[23] Mietzsch M, Jose A, Chipman P, *et al*. Completion of the AAV structural atlas: Serotype capsid structures reveals clade-specific features. Viruses 2021; 13(1): 101. http://dx.doi.org/10.3390/v13010101 PMID: 33450892

[24] Bennett A, Patel S, Mietzsch M, *et al*. Thermal stability as a determinant of AAV serotype identity. Mol Ther Methods Clin Dev 2017; 6: 171-82. http://dx.doi.org/10.1016/j.omtm.2017.07.003 PMID: 28828392

[25] Chhabra A, Bashirians G, Petropoulos CJ, *et al*. Global seroprevalence of neutralizing antibodies against adeno-associated virus serotypes used for human gene therapies. Mol Ther Methods Clin Dev 2024; 32(3): 101273. http://dx.doi.org/10.1016/j.omtm.2024.101273 PMID: 39022744

[26] Gurda BL, DiMattia MA, Miller EB, *et al*. Capsid antibodies to different adeno-associated virus serotypes bind common regions. J Virol 2013; 87(16): 9111-24. http://dx.doi.org/10.1128/JVI.00622-13 PMID: 23760240

[27] Jose A, Mietzsch M, Smith JK, *et al*. High-resolution structural characterization of a new adeno-associated virus serotype 5 antibody epitope toward engineering antibody-resistant recombinant gene delivery vectors. J Virol 2019; 93(1): e01394-18. http://dx.doi.org/10.1128/JVI.01394-18 PMID: 30333169

[28] Tseng YS, Gurda BL, Chipman P, *et al*. Adeno-Associated Virus serotype 1 (AAV1)- and AAV5-antibody complex structures reveal evolutionary commonalities in parvovirus antigenic reactivity. J Virol 2015; 89(3): 1794-808. http://dx.doi.org/10.1128/JVI.02710-14 PMID: 25410874

[29] Klimczak RR, Koerber JT, Dalkara D, Flannery JG, Schaffer DV. A novel adeno-associated viral variant for efficient and selective intravitreal transduction of rat Müller cells. PLoS One 2009; 4(10): e7467. http://dx.doi.org/10.1371/journal.pone.0007467 PMID: 19826483

[30] Devoldere J, Peynshaert K, De Smedt SC, Remaut K. Müller cells as a target for retinal therapy. Drug Discov Today 2019; 24(8): 1483-98. http://dx.doi.org/10.1016/j.drudis.2019.01.023 PMID: 30731239

[31] Wohlschlegel J, Finkbeiner C, Hoffer D, *et al*. ASCL1 induces neurogenesis in human Müller glia. Stem Cell Reports 2023;

18(12): 2400-17.
http://dx.doi.org/10.1016/j.stemcr.2023.10.021 PMID: 38039971

[32] Lee EJ, Kim M, Park S, *et al*. Restoration of retinal regenerative potential of Müller glia by disrupting intercellular Prox1 transfer. Nat Commun 2025; 16(1): 2928.
http://dx.doi.org/10.1038/s41467-025-58290-8 PMID: 40133314

[33] Dalkara D, Kolstad KD, Caporale N, *et al*. Inner limiting membrane barriers to AAV-mediated retinal transduction from the vitreous. Mol Ther 2009; 17(12): 2096-102.
http://dx.doi.org/10.1038/mt.2009.181 PMID: 19672248